Synchrotron Radiation News

ISSN: (Print) (Online) Journal homepage: www.tandfonline.com/journals/gsrn20

Liquid Interface Science at ChemMatCARS

Wei Bu, Binhua Lin, Daniel H. S. Kerr & Mark L. Schlossman

To cite this article: Wei Bu, Binhua Lin, Daniel H. S. Kerr & Mark L. Schlossman (2024) Liquid Interface Science at ChemMatCARS, Synchrotron Radiation News, 37:3, 17-25, DOI: 10.1080/08940886.2024.2351342

To link to this article: https://doi.org/10.1080/08940886.2024.2351342

Liquid Interface Science at ChemMatCARS

Wei Bu,[1] Binhua Lin,[1] Daniel H. S. Kerr,[1] and Mark L. Schlossman[2]
[1]NSF's ChemMatCARS, Pritzker School of Molecular Engineering, University of Chicago, Chicago, IL, USA schloss@uic.edu
[2]Department of Physics, University of Illinois Chicago, Chicago, IL, USA weibu@uchicago.edu

Introduction

Located at Sector 15 of the Advanced Photon Source (APS), ChemMatCARS addresses the need in the USA for facilities and expertise in synchrotron X-ray studies of advanced chemical and materials crystallography, liquid interface science, and anomalous small and wide angle X-ray scattering (Figure 1). Nearly 120 research groups performed X-ray experiments at ChemMatCARS facilities during 2019–2023 to investigate molecular science in areas including chemistry, materials research, biology, and engineering. Here, we focus on studies of liquid surfaces and interfaces carried out at ChemMatCARS. First experiments in the liquid interface program at ChemMatCARS started in 2002 with a user community of four research groups. Advances in the ease of making reliable measurements at ChemMatCARS, and in their analysis, as well as a robust program of outreach activities have led to a cumulative total of 56 research groups. Roughly 20 different research groups use the liquid interface facility during 2-year periods.

Liquid interfaces provide model systems to study the statics and dynamics of interfacial self-assembly, molecular interactions, and chemical reactivity. They provide a platform for the controllable assembly of molecules, ions, or nanoparticles, which dynamically reorganize in response to perturbations, such as changes in pH, bulk phase composition, and interfacial electric fields [1–4]. Synchrotron X-ray surface scattering is a powerful probe of atomic, molecular, and mesoscale structure at liquid interfaces. X-ray scattering studies from liquid surfaces and interfaces have led to key discoveries by users of ChemMatCARS on structures of two-dimensional (2D) molecular and biomolecular films and interfacial ionic ordering [5–17]. Such studies at ChemMatCARS and elsewhere provide information that has changed our understanding of liquid interfacial processes [18].

Liquid interfaces are also used in the preparation and characterization of functional assemblies of surfactants, lipids, polymers, peptides, proteins, liquid crystals, and nanoparticles. These interfacial assemblies exhibit a range of functionalities, including biosensing, optics, drug delivery, signaling, and energy storage [17, 19–26]. Directing the nanoscale assembly of these materials for the purpose of attaining a specific functionality is an ongoing challenge, requiring knowledge of their interfacial

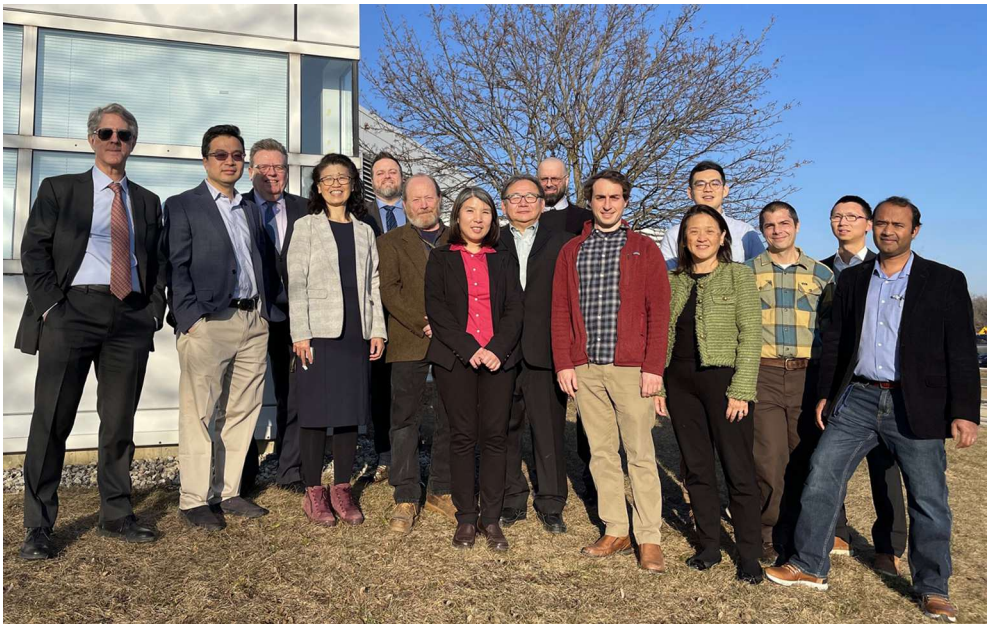

Figure 1: ChemMatCARS principal investigators and staff outside the facility (February 2024). Left to Right: Mark Schlossman, Wei Bu, Matthew Tirrell, Binhua Lin, Jason Benedict, Kevin Lynch, Natalie Chen, Yu-Sheng Chen, Theodore Betley, Daniel Kerr, Ka Yee C. Lee, Tieyan Chang, Ben Stillwell, Jinxing Jiang, Mrinal Bera.

order. To measure the *in situ* molecular-scale ordering of assemblies at liquid interfaces, X-ray surface scattering is often the only viable option.

In this article, we provide a brief overview of technical and scientific activities in liquid interface science at ChemMatCARS. We start with a description of hardware and software capabilities, then describe a few select examples of science in the areas of chemical separations, nanomaterials, life sciences, and bioengineering.

The ChemMatCARS liquid interface facility

The ChemMatCARS liquid interface scattering instrument, with access to a broad range of tunable X-ray energies (5 to 70 keV), allows X-rays to penetrate dense liquids and scatter from buried liquid-liquid interfaces, as well as scatter from liquid-vapor interfaces [27, 28] (Figure 2). The ChemMatCARS facility has placed a high priority on the introduction of "experts-only" techniques to general users who are often novices in the use of synchrotron X-rays. For example, a user-friendly implementation of X-ray fluorescence near total reflection (XFNTR) for the measurement of element-specific interfacial densities was adopted by roughly half of our users within a couple of years. Our development of open-source software over many years has optimized real-time data retrieval, visualization, and analysis for experts and novices alike.

X-ray techniques

Although the ChemMatCARS instrument is capable of the full suite of X-ray surface scattering techniques, the primary techniques in use include X-ray reflectivity (XR) to measure the electron density profile of the interface with sub-nanometer resolution [29–32], grazing-incidence diffraction (GID) to probe ordered molecular or atomic-scale structures within the plane of the surface with sub-angstrom resolution

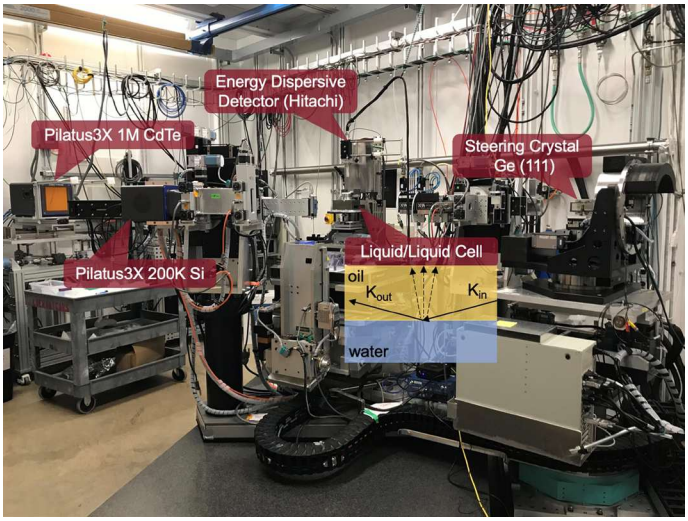

Figure 2: Panoramic view of the ChemMatCARS liquid interface scattering station at the Advanced Photon Source (Argonne National Laboratory, USA). A single steering crystal steers the beam onto the liquid interface. The liquid/liquid cell can be replaced with other sample cells, like a Langmuir trough for measurements of monolayers supported on the water surface. Detector usage is described in the text.

[25, 33–35], and X-ray fluorescence near total reflection (XFNTR) to measure the interfacial density (number per area) of specific elements [5, 13]. Numerous other techniques are in occasional use, including grazing incidence small angle X-ray scattering (GISAXS) and surface diffuse scattering. The kinetics of processes taking place on the order of seconds can be measured with techniques pioneered or further developed at ChemMatCARS. These include fast grazing-incidence diffraction with a 1D pinhole geometry [12, 36, 37] and fast grazing incidence off-specular scattering to measure electron density profiles [12].

Recently, we have commissioned the measurement of X-ray absorption spectroscopy (XAS, including EXAFS and XANES) from liquid surfaces at ChemMatCARS. XAS is the leading technique for measuring elemental speciation in bulk solutions (and in solid state samples), including the identity, number, and distance of coordinating ligands within roughly 5 Å, as well as the elemental oxidation state. The ability to apply this technique to liquid surfaces at a resolution comparable to bulk solution measurements promises to provide substantial new insights by revealing coordination chemistry at the liquid surface.

Detectors

A Si-pixel area detector, Pilatus3X 200K Si, is used for measurements from the liquid-vapor interface; while a CdTe pixel detector, Pilatus3X 1 M CdTe, is used for liquid-liquid interfaces where higher energy X-rays are required [15, 23]. Placing an area detector against the back wall of the experimental hutch, roughly 3 meters from the sample, enables studies of GISAXS from liquid interfaces [38]. An energy dispersive detector (Hitachi Vortex) bundled with fast readout electronics (Xspress3) is used for spectroscopic measurements (Figure 2).

Software

We have found that developing and providing user-friendly, state of the art software for X-ray data collection, reduction, and analysis is critical for the productivity and growth of our user community. We are convinced that our software has accelerated the conversion of data into publishable results, especially for novice users (Figure 3). Rigorous calculation engines and methods for calculating experimental and fitting uncertainties (i.e., error bars) are provided. These include methods of mapping chi-squared space and Markov chain Monte Carlo calculations. By developing this software and training our user community in its use, we have increased the quality of data analysis and expanded the scope of scientific challenges that can be addressed at ChemMatCARS.

A recent development in data analysis for liquid interface scattering is XModFit, a Python-based open-source software designed for extensibility and customization. It is available on the ChemMatCARS website and through GitHub [39]. In addition to providing capabilities for our current techniques, it provides a platform for developing analysis software for new techniques. Python-dependency issues are eliminated by providing compiled versions for our users. Data collection and reduction software, namely LSS_Reader, has been developed to process experimental metadata and large collections of area detector images in real-time into readily usable scattering data [40].

Outreach

ChemMatCARS organizes outreach activities to develop the community of researchers that use synchrotron X-rays to study liquid interfaces. These include an online Soft Matter User Group seminar series that addresses an international audience, schools to train our users in the analysis of X-ray scattering data from liquid interfaces [41, 42], and sponsorship of conference symposia. Recently, ChemMatCARS has sponsored workshops to explore new initiatives in liquid interface science in the areas of biomembranes and cell-surface interactions for biologists, and opportunities to use small X-ray beams to address problems in liquid interfacial engineering.

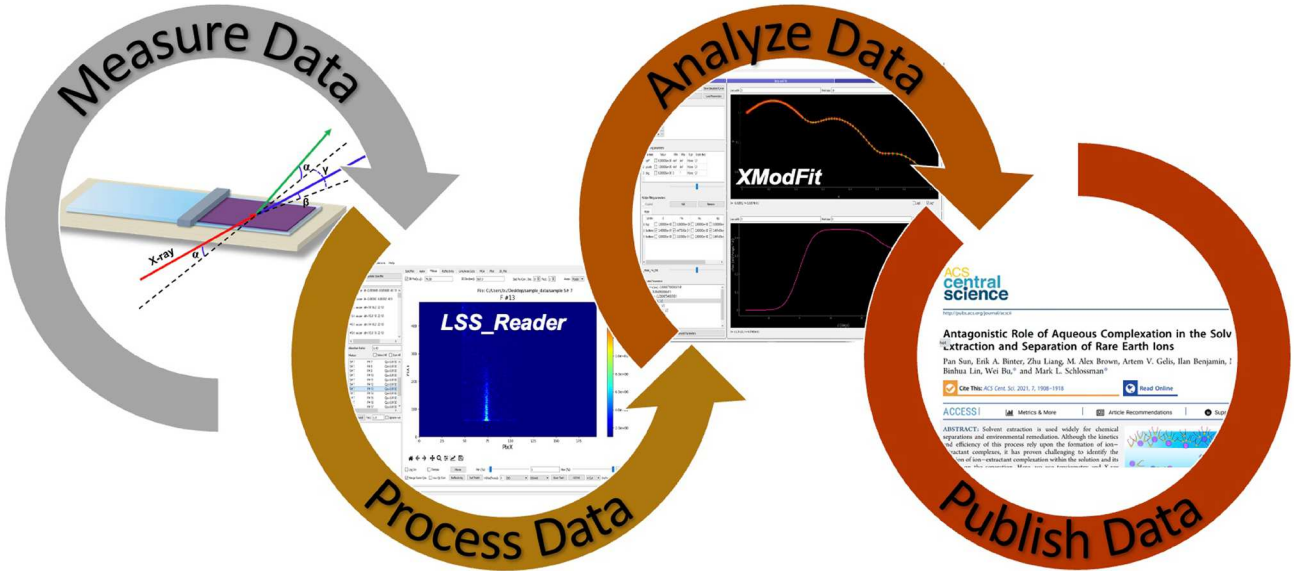

Figure 3: The research workflow for ChemMatCARS users using the liquid interface scattering instrument and software toolkit.

ChemMatCARS runs two diversity outreach programs to expand access to our facility. These include the FaSTRAC program which sponsors faculty/student teams from minority serving (higher education) institutions to do research for a 4 to 6-week period during the summer, as well as the GSRAC program which supports graduate students in carrying out their research and participate in other beamline activities over a 4 to 6-week period during the summer. These programs begin to address the challenge of providing a fuller appreciation of synchrotron X-ray science to graduate students who participate in conventionally brief and hectic synchrotron experiments.

New developments

Synchronous with the accelerator upgrade of the APS, ChemMatCARS is upgrading to convert APS Sector 15 to a two-beamline facility. Canted undulators will feed X-rays concurrently to two beamlines. The ChemMatCARS Sector optics will be replaced entirely, allowing us to take advantage of the small beams, higher brilliance, and higher coherence of the upgraded APS X-ray beam. In addition to maintaining the use of the ChemMatCARS single-crystal-deflector liquid interface instrument, we will install a double crystal deflector (DCD) instrument in a newly constructed station on the second beamline [43–46]. This DCD will have capabilities similar to the DCD instruments at the ESRF in France and at Petra III in Germany, though it will be unique in the U.S. New scientific capabilities will be developed on this instrument that will complement our ongoing program, which we hope to report in a few years.

Liquid interface science at ChemMatCARS

Liquid interfaces are relevant to many technological and environmental challenges. The science described below addresses key questions in the areas of interfacial electrostatics, separations of critical minerals, and the synthesis of 2D and nanomaterials for catalysis and energy applications. Examples will also be drawn from the use of liquid interfaces as model systems for the study of equilibrium and non-equilibrium biomembrane structure on the molecular scale.

Interfacial separation of metallic ions

Electrolyte solutions are the medium for numerous chemical reactions and physical and biological processes. Ions and reactants are often concentrated at interfaces, leading to catalytic, self-assembly, signaling, and separations processes important for fundamental science and industrial commercialization. However, characterizing interfacial ion distributions remains challenging. Recent advances in X-ray interfacial scattering have greatly improved our understanding of interfacial ions and their interactions with other species. ChemMatCARS has a history of contributions in this area, expanding our ability to investigate electrostatics at soft interfaces on a molecular level [15, 38, 47–50] (Figure 4A,B).

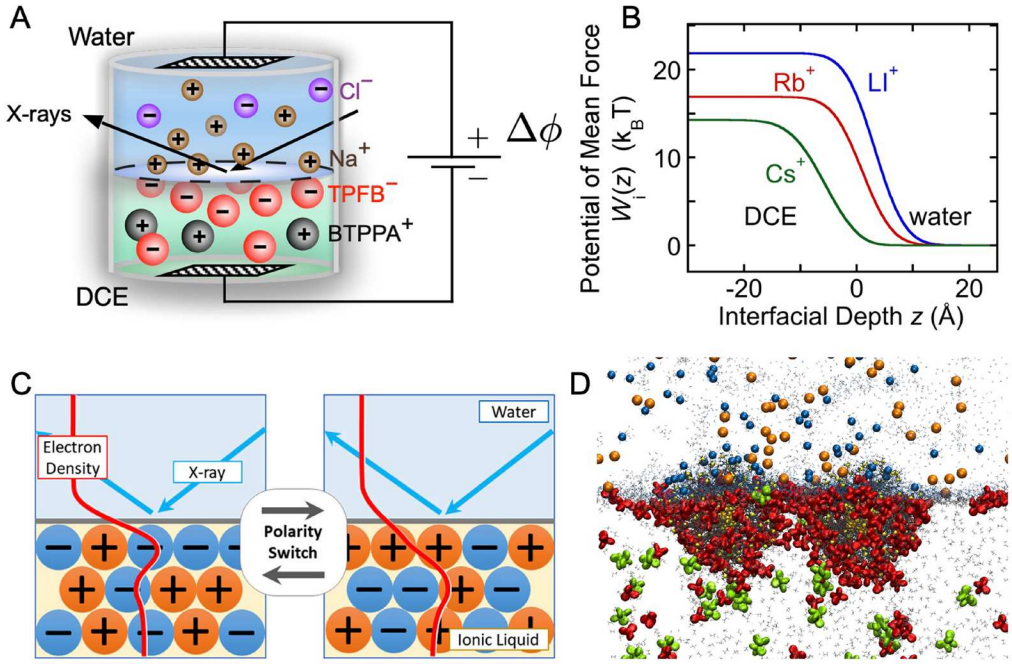

Figure 4: Probing interfacial electrostatics at ChemMatCARS. (A) Illustration of the electrified interface between aqueous and organic electrolyte solutions with ions represented by spheres. Reprinted with permission from Proc. Nat. Acad. Sci. (USA) 109, 20326 (2012). (B) X-ray reflectivity measurements reveal the potentials of mean force for aqueous ions across the aqueous/organic interface. Variation reprinted with permission from J. Phys. Chem. B 117, 5365 (2020). (C) Ionic liquid layering at the aqueous/ionic-liquid interface tuned by the electrochemical potential. Reprinted with permission from J. Phys. Chem. B 124, 6412 (2020). (D) Snapshot of MD simulation that mimics X-ray measurements of charged nanoparticle assemblies at the liquid/liquid interface. Reprinted with permission from Nano Lett. 14, 6816 (2014).

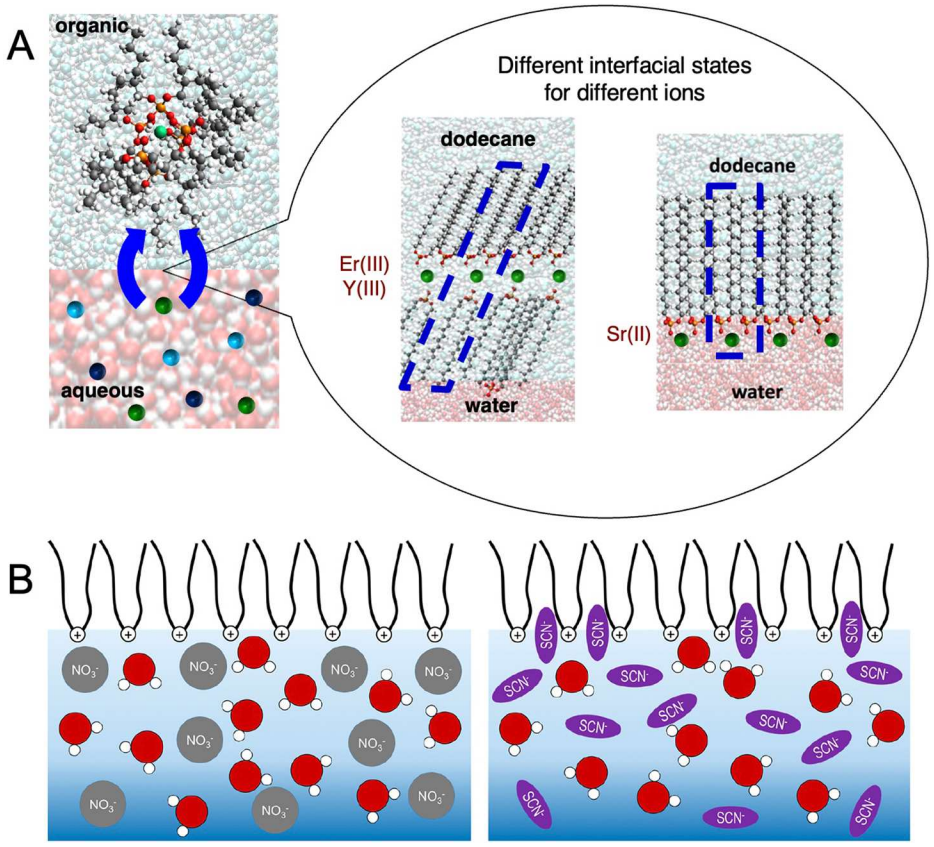

Figure 5: Probing chemical separations at ChemMatCARS. (A) Extractant-assisted transport of ions from aqueous to organic solvents. Interfacial transport mechanism (blue arrows) is under study. X-ray reflectivity and surface fluorescence (XFNTR) reveals different intermediate states trapped at the interface in the midst of extraction. Reprinted with permission from Proc. Nat. Acad. Sci. (USA) 116, 18227 (2019). (B) X-ray study of anion-extractant complexes at the water-vapor interface reveals different configurations for different anions. Reprinted with permission from J. Phys. Chem. C 124, 573 (2020).

Ions and their interactions with amphiphilic extractants at liquid interfaces underlie chemical separations of metals [51]. During the process known as solvent (or liquid-liquid) extraction, extractants and complexants assist the transport of target metal ions across the liquid-liquid interface between an aqueous solution and an organic solvent. Solvent extraction processes are designed to extract a target species of ion from a multi-component aqueous mixture into an organic solvent, then return it to an aqueous phase containing only the targeted species, thereby producing a purified solution of the targeted species. Solvent extraction is used for the removal of toxic metal ions from aqueous sources, the separation and purification of base, precious and rare-earth metals, battery recycling, and the separation of long-lived radionuclides from nuclear waste [51–58].

X-ray measurements at ChemMatCARS have begun to reveal the chemical species that are present at the liquid interface, their arrangement, and the mechanism for ion transport across the liquid-liquid interface, all critical for optimizing the selectivity and kinetics of solvent extraction processes [5, 13, 14, 32, 59–62]. Recent studies at ChemMatCARS by Dutta, Schlossman, Uysal, and co-workers have resulted in discoveries about specific ion effects [13, 14, 59, 60, 63], the role of anions [32, 61, 64], the effect of pH [65], and the counter-intuitive influence of aqueous complexation [14, 63, 66] (Figure 5).

Room temperature ionic liquids are purely ionic without solvent. They are widely investigated in the areas of chemical reactions, separations, and energy storage. Nishi used X-ray reflectivity to study the ionic-liquid/aqueous-electrolyte interface under electrochemical potential control. This revealed the structural development of an ionic multilayer with increasing potential and the growth of alternating cation-rich and anion-rich layers that undergo polarity reversal as the potential is reversed [15] (Figure 4C).

Nanomaterial synthesis at liquid interfaces

Two-dimensional (2D) nanomaterials represent a new direction in materials synthesis with potential applications in the interconversion of electrical and chemical energy, and in quantum materials [67]. The growth of 2D materials on liquid interfaces takes advantage of this essentially defect-free substrate. X-ray studies at ChemMatCARS probe the growth conditions, including the interfacial molecular and ionic environment and *in situ* atomic scale 2D ordering during and after growth. As one example, Michl and Magnera have investigated metallo-

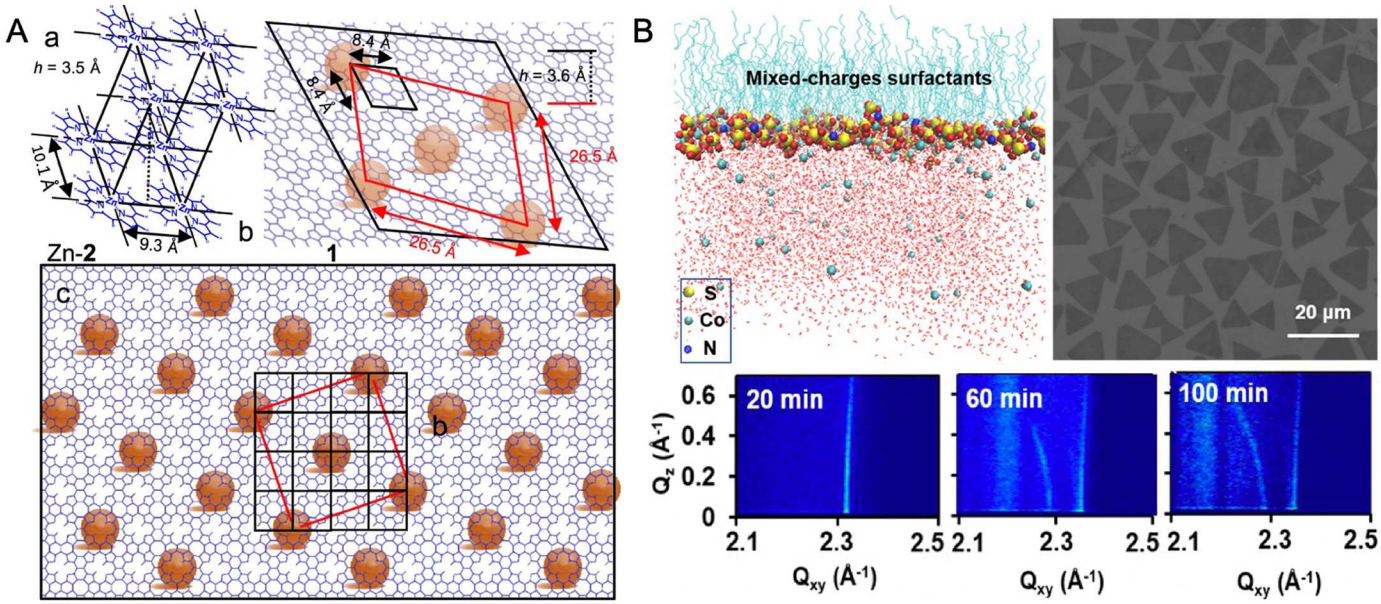

Figure 6: Probing 2D materials synthesis on liquid surfaces at ChemMatCARS. (A) Unit cells at air/water interface from GIXD: (a) unreacted monomer Zn porphyrin, (b) oblique and (c) top view of Zn porphene. Reprinted with permission from Nat. Comm. 14, 6308 (2023). (B) Illustration of the synthesis of ultrathin nanosheet of $Co(OH)_2$ at the water surface by the ILE method. Time-resolved GIXD measurements monitor its structural evolution. Reprinted with permission from Chem. Mater. 31, 9040 (2019).

porphenes, two-dimensional fully conjugated analogs of graphene, whose electrocatalytic properties may be relevant for water oxidation and CO_2 reduction, as well as for their potential as spin-based qubits [68]. One-atom-thick Zn-porphene layers were grown and measured *in situ* at the air-water interface at ChemMatCARS [69] (Figure 6A). Reversible insertion of metal ions suggests that properties of these porphenes can be tuned, and metal centers patterned on the lattice.

Wang has developed ionic layer epitaxy (ILE), a solution interface-based method to synthesize 2D nanomaterials of relevance to electrocatalysis, magnetism, and biomedicine [24, 70–74]. The ILE method employs an ionic surfactant monolayer at the air-solution interface to guide the synthesis (Figure 6B) [34]. The generality of ILE has enabled the growth of 2D nanocrystals of lanthanides, noble metals, hydroxides, and oxides, as well as the direct observation of their growth kinetics at ChemMatCARS [12, 24, 34, 37, 72, 74–76]. Time-resolved grazing-incidence diffraction was used to track the *in-situ* growth of 2D wurtzite ZnO nanosheets at the water surface. These studies led to the discovery of a lateral to vertical growth kinetics switch, which provides synthetic control over the size and thickness of 2D nanocrystals [12].

Tunable nanoparticle arrays

The organized assembly of nanoparticles (NPs) at liquid interfaces has been investigated for the purpose of creating interfaces with specific optical, catalytic, sensing, and electromagnetic functionality [77–81]. The recent development of tunable interfacial assemblies of NPs has the potential to transform the use of nanoparticle arrays by providing remote control over their properties and functionality [38, 82, 83]. Nevertheless, understanding the balance of physical and chemical interactions that determine NP ordering at liquid interfaces remains an open and challenging task. For example, the large electric fields of charged NPs produce strong spatial correlations with counterions and other NPs that are not well understood in the inhomogeneous environment of an interface (Figure 4D) [38]. Vaknin and Wang demonstrated that the influence of salt concentration on PEG phase-separation behavior can be used to order PEG grafted AuNPs on the water surface [83–85]. They are continuing the use of polyethylene glycol (PEG) ligands to build complex colloidal superlattices in an aqueous interfacial environment [9, 20, 86, 87].

Life processes: investigations at liquid interfaces

Interactions between bio-macromolecules, nanoparticles, and cell membranes influence many life processes. Knowledge of the molecular-scale interactions, which determine biological function, is often poor because the disordered nature of biomembrane interfaces is hard to investigate with many biophysical techniques. However, liquid surface X-ray scattering has proven effective in characterizing processes in biomembrane mimics [30, 88–91]. The studies of biomembrane interactions described below have utilized model systems of Langmuir monolayers on the water surface, which appear to be appropriate for processes that involve peripheral membrane proteins. These proteins interact primarily with a single leaflet of the bilayer biomembrane. However, a bilayer model system is required to understand the role of both leaflets of a biomembrane in many processes and Chem-

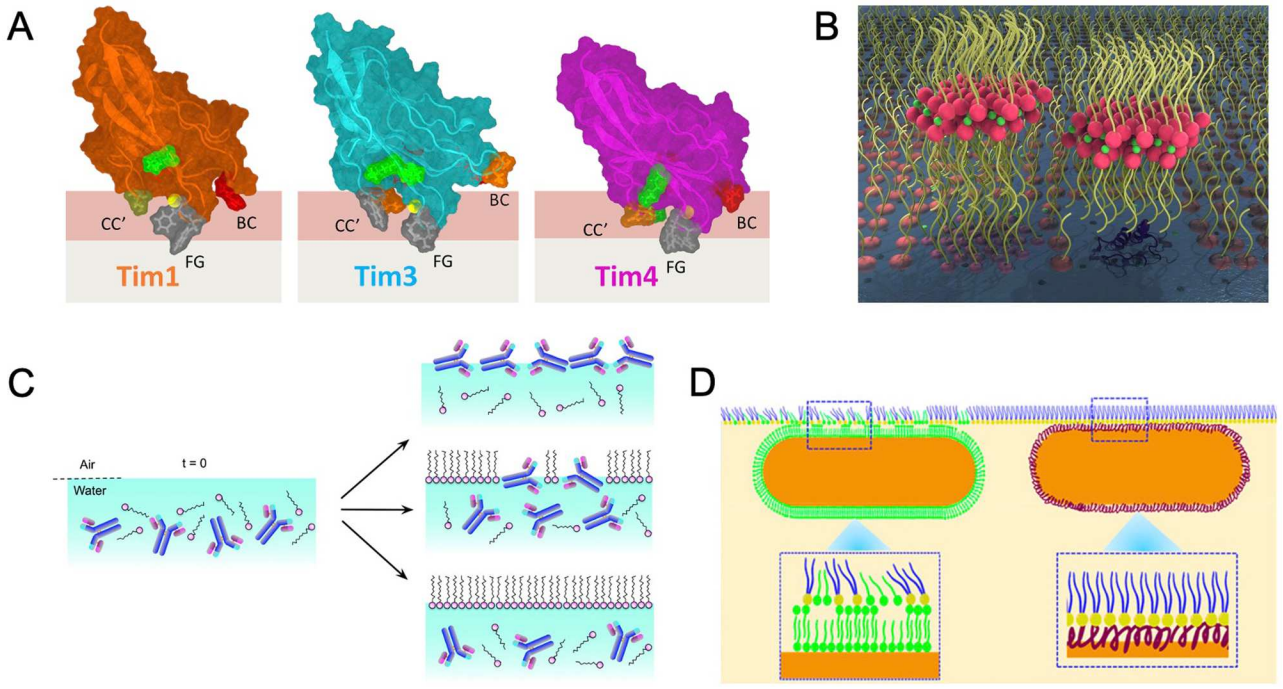

Figure 7: Probing interfacial life processes at ChemMatCARS. (A) Association of Tim proteins with lipid monolayers containing anionic phosphatidylserine. Reprinted with permission from Elsevier Biophysical Journal 120, 4891 (2021). (B) Multilayer degradation products of sPLA$_2$ enzyme-lipid interactions. Reprinted with permission from Soft Matter 15, 4068 (2019). (C) Competition of monoclonal antibodies (mAbs) and surfactant (left) can result in three distinct outcomes, irreversible adsorption of mAbs prevents surfactant adsorption (top right), coadsorption of mAbs and surfactants (middle right), and inhibition of mAbs adsorption by surfactant (bottom right). Reprinted with permission from ACS Appl. Mater. Int. 12, 9977 (2020). (D) Ligand stability regulates the interaction of nanoparticles with biomembranes. Reprinted with permission from ACS Nano 13, 8680 (2019).

MatCARS has plans to establish a facility for bilayer studies at our new beamline.

The complexity of bio-macromolecules has required advances in data analysis techniques. For example, the analysis of X-ray reflectivity to determine the conformation of peripheral membrane proteins bound to a lipid monolayer was originally developed at ChemMatCARS [92, 93]. Further advances in these analysis techniques at ChemMatCARS and in the neutron reflectometry community have incorporated molecular dynamics simulations to account for the flexibility of protein conformations, as well as the analysis of proteins in bilayers [94–96]. As described previously, the development of data analysis software for our users is an integral part of ChemMatCARS' activities and critical to address scientific challenges.

To understand how immune surveillance cells use plasma membrane receptors to recognize phosphatidylserine on activated cells, Lee and co-workers used X-ray reflectivity to study the binding of Tim1, Tim3, and Tim4 (transmembrane immunoglobulin mucin domain proteins) to anionic phospholipid monolayers [95]. Membrane-bound orientations determined by X-ray experiments revealed that each Tim protein interfaces with membranes via a distinct arrangement of chemical moieties on its surface. They found that the proteins differed in how they balanced hydrophobic and electrostatic interactions and in their sensing of phospholipid chain unsaturation and anionic lipid composition (Figure 7A) [95]. The physicochemical differences among the membrane interfaces of the Tim proteins may explain their distinct roles in immunology and sensing of cell membranes.

The protein secretory phospholipase A2 (sPLA$_2$) is overexpressed in various pro-inflammatory diseases and cancers, making it a potential target for diagnosis and treatment. To understand its role better, Liu and co-workers investigated the enzyme-lipid interaction at the water surface with X-ray reflectivity. This revealed the redistribution of sPLA$_2$-induced degradation products into the third dimension, which damaged the original lipid monolayer and produced multilayer domains (Figure 7B). This finding may explain the sPLA$_2$-triggered bursting of liposomes that forms the basis for lipid nanoparticle drug delivery systems [97].

Monoclonal antibodies (mAbs) are the fastest growing biologics used in the treatment of cancers, autoimmune disorders, and infectious diseases [98]. Administering mAbs involves the formation of air-aqueous interfaces, which can lead to adsorption and deactivation due to its inherent hydrophobicity. This can decrease the effective dose and form surface agglomerates [99]. To address this issue, Tu and Maldarelli added surfactants as excipients to compete with mAbs

for surface adsorption (Figure 7C) and demonstrated that the mAbs are unable to adsorb to the surface at sufficiently high levels of excipient [26, 100].

Assessing the safety of engineered nanomaterials in various settings, including environmental, workplace, and medical applications, requires understanding the interactions between nanoparticles and cellular or organelle membranes. Wang examined the impact of coating ligands on membrane adsorption and permeation of nanoparticles. X-ray surface scattering showed that the stability of surface ligands on nanoparticles directly affects the impairment and integrity of cell membranes, which can be linked to the cytotoxicity and immunological effects of nanomaterials (Figure 7D) [31].

Summary

The liquid interface scattering facility at ChemMatCARS is in transition from a single experimental station to two experimental stations. Here, we have reported briefly on the technical capabilities of our single station established by the facility and examples of scientific accomplishments of our user community. These included selections from studies of ions, nanomaterials, and life processes at liquid interfaces. During the roughly 20-year lifetime of the current liquid interface scattering instrument, 169 papers have been published in numerous areas of liquid interface science, most of which we have been unable to mention in this brief overview of ChemMatCARS' activities.

Disclosure statement

The authors report there are no competing interests to declare.

Funding

This work was supported by the National Science Foundation of the United States under grant numbers CHE-1834750 and CHE-1836674 to ChemMatCARS. The Advanced Photon Source, an Office of Science User Facility operated for the U.S. Department of Energy (DOE) Office of Science by Argonne National Laboratory, was supported by the U.S. DOE under Contract No. DE-AC02-06CH11357. ■

ORCID

Wei Bu http://orcid.org/0000-0002-9996-3733
Binhua Lin http://orcid.org/0000-0001-5932-4905
Daniel H. S. Kerr http://orcid.org/0000-0003-1383-2167
Mark L. Schlossman http://orcid.org/0000-0003-3238-1250

References

1. M. Grzelczak et al., *ACS Nano.* **4** (7), 3591 (2010). doi:10.1021/nn100869j
2. Y. Lin et al., *Science.* **299** (5604), 226 (2003). doi:10.1126/science.1078616
3. F. Bresme and M. Oettel, *J. Phys: Condens. Matter* **19** (41), 413101 (2007). doi:10.1088/0953-8984/19/41/413101
4. J. T. Russell et al., *Angew. Chem. Int. Ed.* **44** (16), 2420 (2005). doi:10.1002/anie.200462653
5. Z. Liang et al., *Proc. Natl. Acad. Sci. USA.* **116** (37), 18227 (2019). doi:10.1073/pnas.1701389115
6. C. M. Vander Zanden et al., *Langmuir* **35** (48), 16024 (2019). doi:10.1021/acs.langmuir.9b02484
7. H. Youssef and C. E. DeWolf, *Langmuir* **36** (2), 660 (2020). doi:10.1021/acs.langmuir.9b03120
8. A. Chaudhury et al., *Soft Matter.* **17** (7), 1963 (2021). doi:10.1039/d0sm01945c
9. A. Londoño-Calderon et al., *J. Phys. Chem. C.* **125** (9), 5349 (2021). doi:10.1021/jacs.0c09420 10.1021/acs.jpcc.0c11307
10. W. Bu et al., *Langmuir* **37** (20), 6232 (2021). doi:10.1021/acs.langmuir.1c00420
11. S. K. Singh et al., *Langmuir* **38** (51), 16004 (2022). doi:10.1021/acs.langmuir.2c02462
12. Z. Zhang et al., *Nano Lett.* **22** (7), 3040 (2022). doi:10.1021/acs.nanolett.2c00300
13. M. Miller et al., *Phys. Rev. Lett.* **122** (5), 058001 (2019). doi:10.1103/PhysRevLett.122.058001
14. P. Sun et al., *ACS Cent. Sci.* **7** (11), 1908 (2021). doi:10.1021/acscentsci.1c00960
15. S. Katakura et al., *J. Phys. Chem. B.* **124** (29), 6412 (2020). doi:10.1021/acs.jpcb.0c03711
16. T. Pham et al., *Mol. Pharmaceutic.* **18** (12), 4331 (2021). doi:10.1021/acs.molpharmaceut.1c00494
17. A. Kanthe et al., *Sci. Adv.* **7** (35), eabg2873 (2021). doi:10.1126/sciadv.abg2873
18. P. S. Pershan and M. Schlossman, *Liquid Surfaces and Interfaces: Synchrotron X-Ray Methods* (Cambridge University Press, Cambridge, UK 2012).
19. R. Miclette Lamarche and C. DeWolf, *ACS Appl. Mater. Interfaces* **11** (48), 45354 (2019). doi:10.1021/acsami.9b16958
20. H. J. Kim et al., *ACS Appl. Nano Mater.* **5** (12), 17556 (2022). doi:10.1021/acsanm.2c03042
21. P. Zhang et al., *Langmuir.* **36** (26), 7573 (2020). doi:10.1021/acs.langmuir.0c01202
22. M. Reik et al., *Soft Matter.* **15** (43), 8800 (2019). doi:10.1039/c9sm01579e
23. W. Zhu et al., *Small* **17** (4), 2006279 (2021). doi:10.1002/smll.202006279
24. Z. Zhang et al., *Nano Res.* **13** (12), 3217 (2020). doi:10.1007/s12274-020-2990-7
25. P. Sun et al., *Nano Lett.* **21** (4), 1613 (2021). doi:10.1021/acs.nanolett.0c04147
26. A. D. Kanthe et al., *ACS Appl. Mater. Interfaces* **12** (8), 9977 (2020). doi:10.1021/acsami.9b21979
27. B. Lin et al., *Physica B.* **336** (1-2), 75 (2003). doi:10.1016/S0921-4526(03)00272-2
28. M. L. Schlossman et al., *Rev. Sci. Instrum.* **68** (12), 4372 (1997). doi:10.1063/1.1148399
29. S. R. Clark et al., *Acta Biomater.* **65**, 317 (2018). doi:10.1016/j.actbio.2017.10.027
30. A. M. Fanni et al., *J Biol Chem.* **294** (42), 15304 (2019). doi:10.1074/jbc.RA119.010003
31. L. Wang et al., *ACS Nano.* **13** (8), 8680 (2019). doi: 10.1021/acsnano.9b00114
32. S. Nayak et al., *J. Phys. Chem. Lett.* **11** (11), 4436 (2020). doi:10.1021/acs.jpclett.0c01091
33. J. Kaleta et al., *Proc. Natl. Acad. Sci. USA.* **115** (38), 9373 (2018). doi:10.1073/pnas.1712789115
34. Y. Z. Wang et al., *Chem. Mater.* **31** (21), 9040 (2019). doi:10.1021/acs.chemmater.9b03307
35. J. Rehman et al., *Langmuir.* **35** (32), 10551 (2019). doi:10.1021/acs.langmuir.9b01554

36. M. Meron et al., *Eur. Phys. J. Spec. Top.* **167** (1), 137 (2009). doi:10.1140/Epjst/E2009-00949-0
37. G. Yan et al., *ACS Appl. Mater. Interfaces* **11** (47), 44601 (2019). doi:10.1021/acsami.9b15841
38. M. K. Bera et al., *Nano Lett.* **14** (12), 6816 (2014). doi:10.1021/nl502450j
39. M. K. Bera and W. Bu, *Zenodo.* (2022). doi:10.5281/zenodo.7047225
40. W. Bu, *Zenodo* (2023). doi:10.5281/zenodo.8011600
41. J. M. Andrew et al., *Synchrotron Radiation News* **26** (2), 40 (2013). doi:10.1080/08940886.2013.771076
42. K. Simms et al., *Synchrotron Radiation News* **29** (5), 34 (2016). doi:10.1080/08940886.2016.1220277
43. V. Honkimäki et al., *J. Synchrotron Rad.* **13** (6), 426 (2006). doi:10.1107/S0909049506031438
44. T. Arnold et al., *J. Synchrotron Rad.* **19** (3), 408 (2012). doi:10.1107/S0909049512009272
45. B. M. Murphy et al., *J. Synchrotron Rad.* **21** (1), 45 (2014). doi:10.1107/S1600577513026192
46. O. Konovalov et al., *J. Appl. Crystallogr.* **57** (2), 258 (2024). doi:10.1107/S1600576724000657
47. G. Luo et al., *Science* **311** (5758), 216 (2006). doi:10.1126/science.1120392
48. N. Laanait et al., *Proc. Natl. Acad. Sci. USA.* **109** (50), 20326 (2012). doi:10.1073/pnas.1214204109
49. B. Hou et al., *J. Phys. Chem. B.* **117** (17), 5365 (2013). doi:10.1021/jp401892y
50. B. Hou et al., *J. Electrochem. Soc.* **162** (12), H890 (2015). doi:10.1149/2.0621512jes
51. P. A. Tasker, P. G. Plieger, and L. C. West, in *Comprehensive Coordination Chemistry II: From Biology to Nanotechnology*, edited by J. A. McCleverty and T.J. Meyer (Elsevier, Oxford, 2004), Vol. 9, p. 759.
52. J. Rydberg et al., *Solvent Extraction Principles and Practice*. (Marcel Dekker, New York, NY, 2004).
53. K. L. Nash, in *Separations for the Nuclear Fuel Cycle in the 21st Century ACS Symposium Series 933*, edited by G. J. Lumetta, K. L. Nash, S. B. Clark, and J. I. Friese, (American Chemical Society, Washington, D. C., 2006), pp. 21.
54. Y. A. El-Nadi, *Separation & Purification Reviews* **46** (3), 195 (2017). doi:10.1080/15422119.2016.1240085
55. B. Swain, *J. Chem. Technol. Biotechnol.* **91** (10), 2549 (2016). doi:10.1002/jctb.4976
56. X. Sun, H. Luo, and S. Dai, *Chem. Rev.* **112** (4), 2100 (2012). doi:10.1021/cr200193x
57. S. Lei, W. Sun, and Y. Yang, *J. Hazard. Mater.* **424**, 127654 (2022). doi:10.1016/j.jhazmat.2021.127654
58. M. Kul and K. O. Oskay, *Hydrometallurgy* **155**, 153 (2015). doi:10.1016/j.hydromet.2015.04.021
59. S. Nayak, R. R. Kumal, and A. Uysal, *Langmuir* **38** (18), 5617 (2022). doi:10.1021/acs.langmuir.2c00208
60. S. Yoo et al., *ACS Appl. Mater. Interfaces* **14** (5), 7504 (2022). doi:10.1021/acsami.1c24008
61. K. Lovering et al., *J. Phys. Chem. C.* **124** (1), 573 (2020). doi:10.1021/acs.jpcc.9b09288
62. W. Bu et al., *J. Phys. Chem. B.* **118** (36), 10662 (2014). doi:10.1021/jp505661e
63. P. Sun et al., *J. Phys. Chem. B.* **127** (15), 3505 (2023). doi:10.1021/acs.jpcb.2c08412
64. R. R. Kumal et al., *J. Phys. Chem. C.* **126** (2), 1140 (2022). doi:10.1021/acs.jpcc.1c06925
65. A. J. Carr et al., *ACS Appl. Mater. Interfaces* **14** (51), 57133 (2022). doi:10.1021/acsami.2c16156
66. P. Sun et al., *Proc. Natl. Acad. Sci. USA.* **121** (13), e2315584121 (2024). doi:10.1073/pnas.2315584121
67. M. Asadi et al., *Science* **353** (6298), 467 (2016). doi:10.1126/science.aaf4767
68. A. Urtizberea et al., *Adv. Funct. Materials* **28** (31), 1801695 (2018). doi:10.1002/adfm.201801695
69. T. F. Magnera et al., *Nat. Commun.* **14** (1), 6308 (2023). doi:10.1038/s41467-023-41461-w
70. Y. Zhao et al., *ACS Energy Lett.* **6** (9), 3367 (2021). doi:10.1021/acsenergylett.1c01302
71. G. Yan et al., *ACS Appl. Mater. Interfaces* **13** (44), 52912 (2021). doi:10.1021/acsami.1c14865
72. G. Yan et al., *Nano-Micro Lett.* **12** (1), 49 (2020). doi:10.1007/s40820-020-0387-5
73. X. Yin et al., *Nano Lett.* **19** (10), 7085 (2019). doi:10.1021/acs.nanolett.9b02581
74. X. Yin et al., *Chem. Mater.* **30** (10), 3308 (2018). doi:10.1021/acs.chemmater.8b00575
75. P. Tian et al., *Nanoscale* **10** (11), 5054 (2018). doi:10.1039/C7NR09042K
76. F. Wang et al., *J. Mater. Chem. A.* **5** (19), 9060 (2017). doi:10.1039/C7TA01857F
77. D. Yogev and S. Efrima, *J. Phys. Chem.* **92** (20), 5754 (1988). doi:10.1021/j100331a041
78. E. Smirnov et al., *ACS Nano* **8** (9), 9471 (2014). doi:10.1021/nn503644v
79. H. Duan et al., *Nano Lett.* **5** (5), 949 (2005). doi:10.1021/nl0505391
80. N. Younan et al., *Electrochem. Commun* **12** (7), 912 (2010). doi:10.1016/J.Elecom.2010.04.019
81. S. Crossley et al., *Science* **327** (5961), 68 (2010). doi:10.1126/science.1180769
82. Y. Montelongo et al., *Nature Mater.* **16** (11), 1127 (2017). doi:10.1038/nmat4969
83. H. Zhang et al., *Nanoscale* **9** (1), 164 (2017). doi:10.1039/C6NR07136H
84. H. Zhang et al., *Nanoscale* **9** (25), 8710 (2017). doi:10.1039/C7NR00787F
85. H. Zhang et al., *J. Phys. Chem. C.* **121** (28), 15424 (2017). doi:10.1021/acs.jpcc.7b02549
86. H. J. Kim et al., *ACS Appl. Nano Mater.* **3** (8), 8216 (2020). doi:10.1021/acsanm.0c01643
87. W. Wang et al., *Langmuir* **36** (1), 311 (2020). doi:10.1021/acs.langmuir.9b02966
88. J. Y. Wang et al., *Biomacromolecules* **20** (9), 3385 (2019). doi:10.1021/acs.biomac.9b00621
89. F. R. Dayeen et al., *Biophys J* **121** (18), 3533 (2022). doi:10.1016/j.bpj.2022.07.007
90. R. P. Giri et al., *J. Phys. Chem. Lett.* **13** (49), 11430 (2022). doi:10.1021/acs.jpclett.2c02971
91. J. Yu et al., *Soft Matter* **16** (4), 983 (2020). doi:10.1039/c9sm01642b
92. Š. Málková et al., *Biophys. J* **89** (3), 1861 (2005). doi:10.1529/biophysj.105.061515
93. C.-H. Chen et al., *Biophys. J.* **97** (10), 2794 (2009). doi:10.1016/j.bpj.2009.08.037
94. G. T. Tietjen et al., *Biophys. J.* **113** (7), 1505 (2017). doi:10.1016/j.bpj.2017.08.003
95. D. Kerr et al., *Biophys. J.* **120** (21), 4891 (2021). doi:10.1016/j.bpj.2021.09.016
96. F. Heinrich and M. Lösche, *Biochimica Et Biophysica Acta Bba - Biomembr* **1838** (9), 2341 (2014). doi:10.1016/j.bbamem.2014.03.007
97. P. Zhang et al., *Soft Matter* **15** (20), 4068 (2019). doi:10.1039/c8sm01154k
98. Q. Zhang et al., *Cell Res.* **17** (2), 89 (2007). doi:10.1038/sj.cr.7310143
99. M. Vázquez-Rey and D. A. Lang, *Biotech. Bioeng.* **108** (7), 1494 (2011). doi:10.1002/bit.23155
100. A. D. Kanthe et al., *Mol. Pharmaceutic.* **19** (9), 3100 (2022). doi:10.1021/acs.molpharmaceut.2c00152